Serum response factor and myocardin mediate arterial hypercontractility and cerebral blood flow dysregulation in Alzheimer's phenotype

Nienwen Chow*, Robert D. Bell*, Rashid Deane†, Jeffrey W. Streb‡, Jiyuan Chen‡, Andrew Brooks§, William Van Nostrand¶, Joseph M. Miano‡, and Berislav V. Zlokovic†‖

*Socratech Research Laboratories L.L.C., †Frank P. Smith Laboratories for Neuroscience and Neurosurgical Research, Department of Neurosurgery, ‡Cardiovascular Research Institute, and §Functional Genomics Core, Arthur Kornberg Medical Research Building, University of Rochester School of Medicine, 601 Elmwood Avenue, Rochester, NY 14642; and ¶Department of Medicine, Stony Brook University, Stony Brook, NY 11794

Edited by Eric N. Olson, University of Texas Southwestern Medical Center, Dallas, TX, and approved November 21, 2006 (received for review September 19, 2006)

Cerebral angiopathy contributes to cognitive decline and dementia in Alzheimer's disease (AD) through cerebral blood flow (CBF) reductions and dysregulation. We report vascular smooth muscle cells (VSMC) in small pial and intracerebral arteries, which are critical for CBF regulation, express in AD high levels of serum response factor (SRF) and myocardin (MYOCD), two interacting transcription factors that orchestrate a VSMC-differentiated phenotype. Consistent with this finding, AD VSMC overexpressed several SRF-MYOCD-regulated contractile proteins and exhibited a hypercontractile phenotype. *MYOCD* overexpression in control human cerebral VSMC induced an AD-like hypercontractile phenotype and diminished both endothelial-dependent and -independent relaxation in the mouse aorta *ex vivo*. In contrast, silencing *SRF* normalized contractile protein content and reversed a hypercontractile phenotype in AD VSMC. *MYOCD in vivo* gene transfer to mouse pial arteries increased contractile protein content and diminished CBF responses produced by brain activation in wild-type mice and in two AD models, the Dutch/Iowa/Swedish triple mutant human amyloid β-peptide (Aβ)-precursor protein (*APP*)-expressing mice and *APPsw*$^{+/-}$ mice. Silencing *Srf* had the opposite effect. Expression of SRF did not change in VSMC subjected to Alzheimer's neurotoxin, Aβ. Thus, SRF-MYOCD overexpression in small cerebral arteries appears to initiate independently of Aβ a pathogenic pathway mediating arterial hypercontractility and CBF dysregulation, which are associated with Alzheimer's dementia.

cerebral vasculature | dementia | smooth muscle | differentiation

Alzheimer's dementia is characterized by the progressive cognitive decline and chronic neurodegenerative process associated with neurovascular dysfunction (1, 2). There is increasing recognition that cerebrovascular disease contributes to cognitive impairment and dementia (3–5). Arterial hypoperfusion and cerebral blood flow (CBF) dysregulation may precede cerebral atrophy and brain accumulation of Alzheimer's neurotoxin, amyloid β-peptide (Aβ), in animal models of Alzheimer's disease (AD; refs. 6–8) and in AD individuals (9–11). The CBF reductions may in turn impair protein synthesis (12), which is required for learning and memory (13, 14), and precipitate ischemic injury in AD (15, 16). In its final stages, cerebral Alzheimer's arteriopathy is associated with Aβ deposition known as cerebral amyloid angiopathy, which may result in vascular smooth muscle cell (VSMC) death with lobar hemorrhages (3).

The molecular and cellular basis of Alzheimer's arteriopathy is poorly understood. Here, we report that two interacting transcription factors that orchestrate a VSMC-differentiated phenotype, the serum response factor (SRF) and myocardin (MYOCD; ref. 17), are overexpressed in AD VSMC and elicit a hypercontractile VSMC phenotype in AD through directed expression of SRF/MYOCD-regulated contractile genes. This hypercontractile state, in turn, appears to initiate a pathogenic pathway mediating Alzheimer's cerebral arterial hypercontractility, CBF reductions, and decreased CBF responses to brain activation contributing to cognitive decline. These data provide important transcriptional insight into a possible mechanism for the development of Alzheimer's vascular disorder associated with dementia in humans.

Results

We analyzed VSMCs derived from small cortical pial and intracerebral arteries from eight late-stage AD patients with severe pathology, five neurologically normal nondemented age-matched controls with no or sparse pathology, and five young controls with no pathology [see *Methods* and supporting information (SI) Tables 1 and 2]. First, we noted in a microarray screen that a subset of genes encoding for VSMC-restricted proteins was abundantly represented in AD compared with controls (data not shown). Western blotting demonstrated elevated levels of VSMC-restricted contractile proteins in AD VSMC compared with age-matched VSMC (Fig. 1 *a* and *b*). A large number of VSMC-restricted genes are regulated by SRF, a transcription factor that binds a 1,216-fold degenerate cis element known as a CArG box (18). The levels of full length SRF were substantially higher in AD VSMC compared with controls (Fig. 1 *a* and *c*). In some experiments, lower-molecular-weight SRF species (Fig. 1*a*), which may correspond to spliced or caspase-mediated cleaved SRF, as shown in the failing heart (19), were also present. These SRF variants could act as dominant-negative SRF isoforms (19–21).

SRF binds a cardiac- and VSMC-restricted coactivator MYOCD (22). Together, SRF MYOCD potently activates a program of SMC differentiation (23–26). Fig. 1 *a* and *d* show that AD VSMC express nearly 2.7-fold higher levels of MYOCD protein and substantially higher levels of *MYOCD* mRNA compared with controls, respectively. The Western

Author contributions: N.C., R.D.B., R.D., and J.W.S. contributed equally to this work; J.M.M. and B.V.Z. designed research; N.C., R.D.B., R.D., J.W.S., J.C., and A.B. performed research; J.W.S. and W.V.N. contributed new reagents/analytic tools; N.C., R.D.B., R.D., J.W.S., A.B., J.M.M., and B.V.Z. analyzed data; and B.V.Z. wrote the paper.

Conflict of interest: B.V.Z. is the scientific founder of Socratech L.L.C., a startup biotechnology company with a mission to develop neuroprotective strategies in the aging brain and for brain disorders such as stroke, Alzheimer's disease, and other neurodegenerative disorders. All other authors declare no conflict of interest.

This article is a PNAS direct submission.

Abbreviations: AD, Alzheimer's disease; CBF, cerebral blood flow; VSMC, vascular smooth muscle cell; SRF, serum response factor; MYOCD, myocardin; Aβ, amyloid β-peptide.

‖To whom correspondence should be addressed. E-mail: berislav_zlokovic@urmc.rochester.edu.

This article contains supporting information online at www.pnas.org/cgi/content/full/0608251104/DC1.

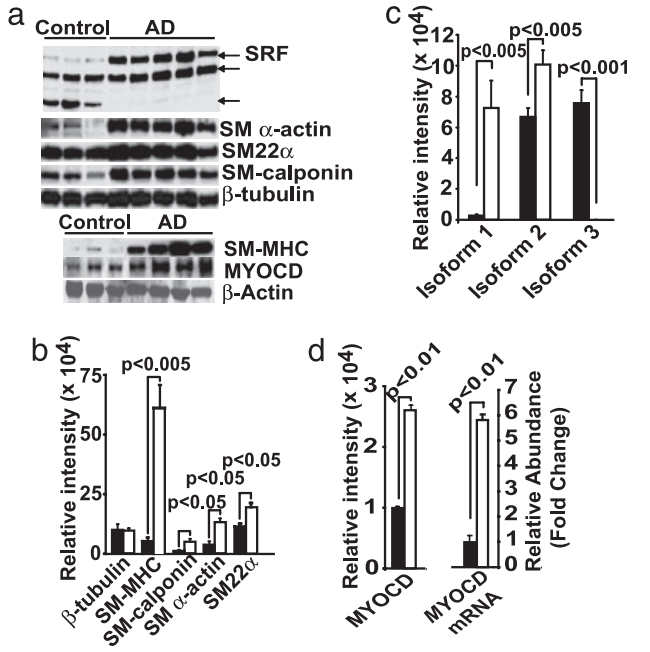

Fig. 1. SRF/MYOCD and contractile protein expression in Alzheimer's cerebral VSMC. (*a*) Shown are Western blots of a full length SRF, SM α-actin, SM22α, and SM calponin (*Upper*) and of smooth muscle myosin heavy chain (SM MHC) and MYOCD (*Lower*) in AD and age-matched control VSMC. (*b* and *c*) Relative levels of expression of VSMC contractile proteins (*b*) and SRF (*c*) in AD (open bars) and controls (filled bars). (*d*) Relative levels of expression of MYOCD (*Left*) and quantitative RT-PCR for *MYOCD* mRNA (*Right*) in VSMC in AD (open bars) and controls (filled bars). Mean ± SEM from five to eight independent cultures per group. *P*, statistically significant difference between AD vs. controls.

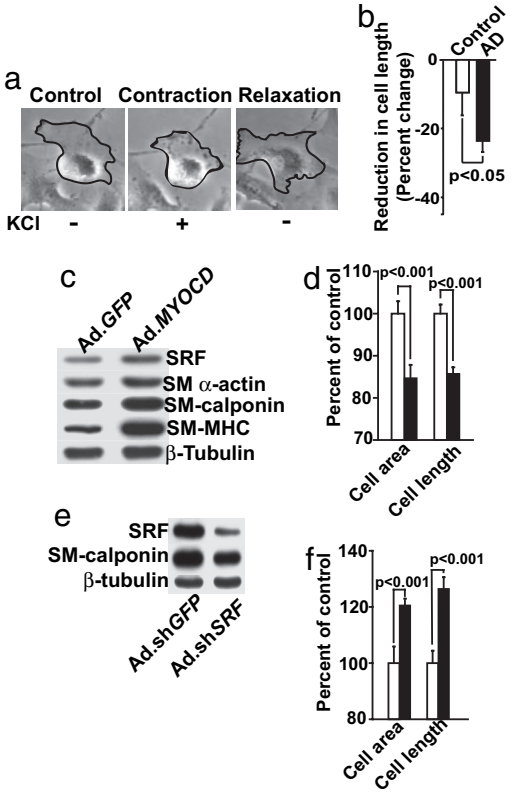

Fig. 2. VSMC contractility in response to KCl. (*a*) Cerebral control VSMC before (control), during (contraction), and after (relaxation) stimulation with KCl. (*b*) Contractility of AD VSMC vs. control VSMC after KCl stimulation. Mean ± SEM are from eight AD and five age-matched independent cultures. *P*, statistically significant difference. (*c* and *d*) Western blot analysis for SRF, SM α-actin, SM calponin, and SM MHC (*c*) and VSMC contractility after stimulation with KCl in *MYOCD*- (Ad.*MYOCD*) (filled bars) or Ad.*GFP*-transduced (control) age-matched VSMC (open bars) (*d*). (*e*) Western blots for SRF and SM calponin and (*f*) VSMC contractility after KCl stimulation in AD VSMC transduced with Ad.sh*SRF* (filled bars) or control Ad.sh*GFP* (open bars). Western blots in *c* and *e* are typical representatives of five independent experiments from five different cultures per group. In *d* and *f*, the maximal cell shortening was determined from 100 cells per culture in triplicates from three independent cultures per group (mean ± SEM); *P*, statistically significant difference between *MYOCD*- vs. *GFP*-transduced VSMC and sh.*SRF*- vs. sh.*GFP*-transduced AD VSMC, respectively, determined by Student's *t* test.

blot analysis of microvascular homogenates prepared from isolated intracerebral and leptomeningeal small arteries confirmed that AD cases, compared with controls, express significantly higher levels of SRF, SM calponin, SM α-actin, and SM MHC (data not shown). These results suggest the increases in SRF and several VSMC contractile proteins in AD VSMC arise from MYOCD acting over each gene's set of functional CArG regulatory elements (18).

Because the expression of contractile proteins was increased in AD VSMC (Fig. 1), we hypothesized that the contractile activity of AD VSMC may also be higher compared with age-matched controls. Fig. 2*a* shows a shortening (contraction) of control human VSMC in response to potassium chloride (KCl), with a maximal effect at 5–10 min after KCl administration and a slow return to precontraction dimensions (relaxation) (SI Movie 1). This contractile competence was not the result of cellular stress, because no significant increase in lactate dehydrogenase release was observed (data not shown). Moreover, phalloidin staining 10 min after KCl exposure showed rearrangements of actin stress fibers typifying a contractile state (data not shown). Cultured VSMC are generally refractory to contractile stimulation because of their phenotypic modulation, which may explain the relatively slow contraction and relaxation of cerebral VSMC *in vitro* compared with their rapid responses *in vivo* (2). An analysis of multiple independent cultures of VSMC (the same ones used in Fig. 1) demonstrated a statistically significant increase ($P < 0.05$) in KCl-induced cell shortening in AD VSMC compared with control VSMC, i.e., 24.5% vs. 9.2%, respectively (Fig. 2*b*). For details regarding the time-dependent response of VSMC to KCl, the requirement of extracellular calcium ions for contraction, and calcium fluxes in response to KCl in control and AD VSMC, see SI Fig. 5.

Because increased MYOCD expression was associated with elevated contractile protein expression and contractility in AD VSMC, we hypothesized that overexpressing *MYOCD* gene in normal cerebral VSMC would augment contractile protein expression and activity leading to an AD-like hypercontractile phenotype. Adenoviral-mediated transfer of human *MYOCD* gene increased, dose-dependently, *MYOCD* mRNA expression in normal VSMC (not shown) and augmented significantly the levels of SRF and contractile proteins SM MHC, SM calponin, and SM α-actin (Fig. 2*c*), consistent with earlier reports (25, 26). Moreover, *MYOCD* gene transfer resulted in increased VSMC contractility compared with *GFP* controls (Fig. 2*d*). In contrast, silencing *SRF* in AD VSMC with adenoviral-mediated transfer of short-hairpin *SRF* RNA (Ad.sh*SRF*) reduced the expression of SRF by ≈70%, as well as the expression of SRF-dependent VSMC contractile protein SM calponin (Fig. 2*e* and SI Fig. 6*a*), consistent with our observation that Ad.sh*SRF* effectively reduces endogenous SRF levels and the expression of *SRF* target genes in various cell lines (27, 28). Silencing the *SRF* gene also reduced hypercontractility of AD VSMC (Fig. 2*f*).

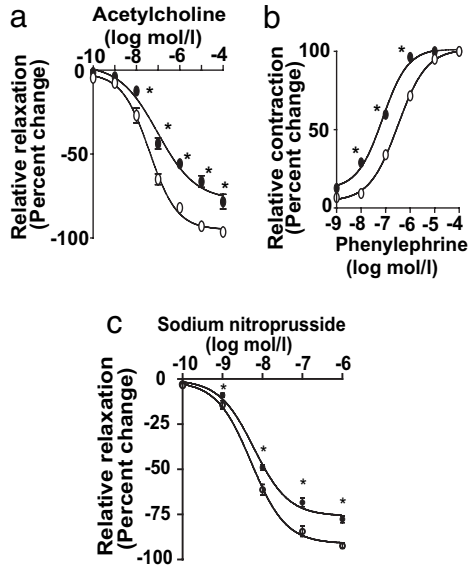

Fig. 3. SRF/MYOCD regulate contractile phenotype in mouse aortic rings. Cumulative dose–response curves for acetylcholine (*a*), phenylephrine (*b*), and sodium nitroprusside (*c*) in mouse aortic rings transduced with Ad.*MYOCD* (solid circle) or Ad.*GFP* (open circle). Mean ± SEM from three rings per group; *, $P < 0.05$, *MYOCD*- vs. *GFP*-transduced by Student's *t* test.

To determine whether our findings in cultured VSMC translate to a mouse model, we transduced *ex vivo* mouse aortic rings with *MYOCD* gene or *GFP* and studied the responses of transduced vessels (SI Fig. 6*b Inset*) to acetylcholine, an endothelial-dependent vasodilator that increases nitric oxide production, and phenylephrine, a direct VSMC vasoconstrictor (29). Fig. 3 *a* and *b* show shifts to the right and left of the respective acetylcholine-induced arterial relaxation curve and phenylephrine-induced contraction curve in *MYOCD*-transduced vessels compared with *GFP*-transduced controls, suggesting that *MYOCD* gene transfer reduces arterial vasodilation and amplifies arterial contractility. The effects of sodium nitroprusside (SNP), a nitric oxide donor that causes endothelial-independent VSMC relaxation (29), were tested in vessels denuded of endothelium. Fig. 3*c* shows that SNP-mediated relaxation of Ad.*MYOCD*- transduced rings was significantly ($P < 0.05$) attenuated compared with *GFP* controls. Consistent with these findings, we found a 2.2-fold increase in SM MHC levels in *MYOCD*-transduced vessels (SI Fig. 6*b*).

We next asked whether altering SRF/MYOCD expression in VSMC of cerebral arteries *in vivo* would modulate neocortical CBF responses to somatosensory stimulation in wild-type mice and in two animal models of AD. Genetic inactivation of *Myocd* or conditional knockout of *Srf* results in embryonic lethality because of cardiovascular defects (30, 31), and *Srf* overexpression results in severe cardiac abnormalities and death (32), thus precluding loss- or gain-of-function studies in context of AD cerebrovascular pathology. Therefore, we used a slow subarachnoid colony-stimulating-factor perfusion technique for adenoviral-mediated *MYOCD* or sh*SRF* gene transfer to mouse subarachnoid pial neocortical arteries (for details, see *Methods* and *SI Text*). Fig. 4 *a–c* illustrate efficient gene transfer to the VSMC layer of pial arteries at the surface of the mouse brain, as indicated by GFP, expression of *MYOCD* mRNA, and a substantial increase in VSMC contractile protein content in Ad.*MYOCD*-transduced arteries compared with Ad.*GFP* controls. Whisker stimulation (7, 8) in control mice transduced with Ad.*GFP* increased CBF by ≈35%, which was only somewhat lower than in wild-type mice, whereas *MYOCD* overexpression

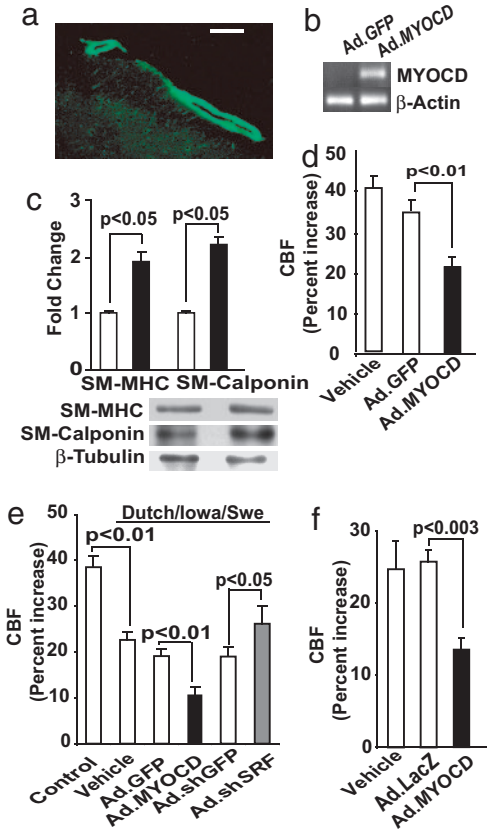

Fig. 4. *MYOCD* and sh.*SRF* gene transfer to mouse pial arteries alters CBF responses to vibrissal stimulation. (*a*) Expression of GFP in cerebral pial vessels after subarachnoid infusion of Ad.*GFP*. (Scale bar, 50 μm.) (*b*) PCR for *MYOCD* mRNA in cerebral pial vessels after *in vivo* transduction with Ad.*MYOCD*. (*c*) Increase in contractile protein content in cerebral pial arteries after *MYOCD* gene transfer compared with *GFP* controls by Western blot analysis. (*d–f*) Effect of *MYOCD* gene transfer on CBF increase after whisker stimulation compared with *GFP* controls in wild-type (*d*), Dutch/Iowa/Swe (*e*), and *APPsw*$^{+/-}$ mice (*f*). In *d–f*, mock colony-stimulating-factor controls (vehicle) were also studied. Mean ± SEM from five animals per group.

significantly ($P < 0.01$) reduced CBF increase to 21%, which was 57% of the CBF increase observed in *GFP* controls (Fig. 4*d*).

Next, we studied whether *MYOCD* gene transfer to neocortical pial arteries disrupts CBF regulation in the Dutch/Iowa/Swedish triple mutant human *APP*-expressing mice, which develop rapid, robust, and early Aβ accumulations in the brain and vasculature (33). Our data show reduced CBF response to whisker stimulation in 9-mo-old Dutch/Iowa/Swedish mice, i.e., 21% vs. 38% increase in the littermate controls (Fig. 4*e*), as expected because of vasoconstrictor properties of Aβ (1, 2, 7, 8). The CBF increase in response to vibrissal stimulation in the Dutch/Iowa/Swedish mice was not affected significantly by *GFP* transduction (control) but dropped to 10% after *MYOCD* gene transfer, representing a 50% decrease from *GFP* controls. The CBF increased to 27% after sh*SRF* gene transfer, compared with 19% in sh*GFP* controls, which was an ≈40% increase (Fig. 4*e*). Although Dutch and Iowa Aβ mutations occur individually in familial forms of AD with cerebrovascular pathology (33), the double mutation has not been identified in humans. To show that our findings are not restricted to the Dutch/Iowa/Swedish model of AD, we performed similar studies in *APPsw*$^{+/-}$ mice, which develop significant cerebral amyloid angiopathy after 12 mo of age (34). Fig. 4*f* shows that *MYOCD* gene transfer to neocortical pial vessels in 16-mo-old *APPsw*$^{+/-}$ mice significantly ($P < 0.01$) reduced the CBF increase in response to vibrissal stimulation. Taken together, these studies validate func-

tional changes in CBF of AD models stemming from altered expression of SRF/MYOCD.

Finally, to test whether a link exists between Aβ vascular deposition and SRF expression, we studied the effects of Aβ on SRF expression. Exogenous Aβ42 at different concentrations and structural forms (e.g., oligomers, aggregates; ref. 35) and over incubation times within 72 h did not affect SRF expression in cultured human cerebral VSMC (SI Fig. 7). Thus, we conclude that the increase in SRF observed in AD VSMC is not a consequence of accumulated Aβ peptides.

Discussion

Accumulating clinical evidence supports a critical role for vascular hypoperfusion in AD dementia (1–5, 11), although the molecular basis for this important vascular defect is unclear. We now report an exaggerated level of SRF/MYOCD expression in VSMC derived from cerebral vessels of AD patients. Such increases in SRF/MYOCD appear to underlie elevations in expression of contractile proteins that correlated with a hypercontractile phenotype in AD VSMC. It is of note that our study was focused on VSMC derived from human small pial and intracerebral arteries, which offer the greatest resistance to CBF and play a major role in rapid CBF responses during brain activation (1, 2). We further show MYOCD overexpression in normal human cerebral VSMC phenocopies the AD VSMC state, with increases in contractile protein content and hypercontractility. As expected, we also found increased expression of some of the SRF-dependent genes that regulate Ca^{2+} homeostasis, e.g., myosin light-chain kinase (*MYLK*), calsequestrin 1 (*CASQ1*), and sarcoplasmic/endoplasmic reticulum calcium ATPase 2 (*ATP2A2*) (SI Fig. 8), which might also contribute to observed hypercontractility in addition to changes in expression of structural contractile proteins.

MYOCD overexpression in mouse aorta and in cerebral arterial pial vessels in wild-type mice and two AD mouse models resulted in diminished endothelial-dependent and -independent relaxation and reduced brain activation-induced increases in CBF, respectively. Although MYOCD can elicit a near-complete program of VSMC differentiation (36), it has been unclear whether MYOCD *per se* can promote VSMC contractility (37). Our data suggest that MYOCD can direct a functional contractile state in human cerebral VSMC, which resembles an AD-like hypercontractile VSMC phenotype. In contrast, *SRF* silencing has an opposing effect on the AD VSMC hypercontractile phenotype. These studies provide potential molecular insight into the well defined hypoperfused brains of patients with AD dementia.

A myriad of factors may contribute to the cerebrovascular alterations in AD (1, 2). We have recently demonstrated that dysregulation of the mesenchyme homeobox gene 2 (*MEOX2*) in brain capillary endothelium plays a major role in dysfunction of brain capillary unit in AD (38). However, *MEOX2* homeoprotein was not significantly altered in AD cerebral VSMC (data not shown), and our ongoing studies suggest no relationship between MEOX2 and SRF/MYOCD transcription factors in the context of AD vascular disorder. We also ruled out Aβ as the upstream factor responsible for SRF up-regulation, as indicated by studies in cultured VSMC. Sublethal concentrations of Aβ42 may lower SRF activity in cultured neurons (39), but the pathophysiological significance of this finding remains unclear. Although SRF is expressed in neurons and plays a role in neuronal migration and axon guidance (40) and learning (41), the observed changes in SRF/MYOCD are likely to be specific for VSMC, because MYOCD expression is restricted to the heart and SMCs (17).

Brains of AD patients are frequently exposed to chronic hypoxia (1, 2, 4, 5, 11). Hypoxia may enhance expression of MYOCD in VSMC precursor cells (42). Our ongoing studies indicate hypoxia increases the levels of MYOCD mRNA in cultured VSMC (SI Fig. 9) associated with increased levels of SRF (not shown). This finding raises a possibility that hypoxic conditions in AD brains caused by atherosclerosis of larger cerebral arteries (1, 5, 43) might contribute to SRF/MYOCD overexpression in VSMC in small pial and intracerebral downstream arteries resulting in CBF dysregulation and reductions (9–11). Because oxidant stress plays a role in Aβ-induced cerebrovascular dysfunction through NADPH oxidase-derived reactive oxygen species (44), we also studied whether oxidant stress increases the activity of the SRF/MYOCD pathway. Our results in cultured SMC indicate no changes in promoter activity of SRF-dependent genes SM22α, SM α-actin, or SM calponin in response to H_2O_2-induced oxidant stress in the presence or absence of MYOCD (SI Fig. 10), suggesting oxidant stress is not upstream to the SRF/MYOCD at least under *in vitro* conditions in the SMC studied. These findings are consistent with our observations in human leptomeningeal SMC showing that Aβ also does not affect expression of SRF (SI Fig. 7). The present data do not rule out the possibility that there may be genetic polymorphisms in regulatory regions of *SRF*/*MYOCD* transcription factors in AD patients, which may result in elevated levels of SRF and MYOCD in AD.

In summary, we suggest elevated SRF/MYOCD activity may promote a hypercontractile VSMC phenotype in small brain arteries, which could initiate pathology underlying brain hypoperfusion and neurovascular uncoupling commonly seen in AD. Thus, SRF/MYOCD could be novel targets for treating arterial cerebral dysfunction associated with cognitive decline in AD.

Methods

Participants and Neuropathological Diagnosis. VSMC from small cortical pial arteries (areas 9/10) were rapidly isolated from 18 individuals upon autopsy. AD patients and age-matched controls were evaluated clinically and followed to autopsy at the AD Research Centers at the University of Southern California and the University of Rochester Medical Center. The Clinical Dementia Rating scores in AD and control individuals were 3–5 and 0, respectively. AD cases were Braak stage V–VI (45) and Consortium to Establish Registry for Alzheimer's Disease (CERAD) (46), frequent to moderate. Controls were Braak 0 or 0–I and CERAD, negative or sparse. The incidence of vascular risk factors (e.g., hypertension, atherosclerosis, etc.), gender ratio, age, cause of death, and postmortem interval (PMI) was comparable between AD and age-matched controls. The PMI ranged between 2.8 and 6 h. VSMCs from young controls (average age 31.2 years) were isolated from rapid brain autopsies of neurologically normal young individuals with no vascular risk factors autopsied after motor vehicle accidents at the Monroe Medical Examiner Center, Rochester, NY. The cells were harvested under an approved Western Institutional Review Board (WIRB), Protocol no. 1534 WIRB; Study no. 1028052, "Human Autopsy Tissue Research Protocol."

Human VSMC Culture. Arterial VSMCs were isolated from pial cerebral arteries and characterized as reported (47). In all studies, we used passage 4 VSMCs.

Western Blotting. VSMCs were washed in cold phosphate buffer saline, lysed with "crack" buffer, and processed for Western blot analysis (22, 27, 31). For details on antibodies and procedures, see *SI Text*.

Quantitative PCR. We performed mRNA quantification using TaqMan chemistry with fluorescently tagged oligonucleotide probes (48). The following primers were used for *MYOCD* (268 bp): sense, 5′-TTTCAGAGGTAACACAGCCTCCATCC-3′, and antisense, 5′-ACTGTCGGTGGCATAGGGATCAAA-3′. The amplified product represents the 3′ untranslated region of human MYOCD, which has not been completely annotated in databases.

VSMC Contractile Competence Assay. VSMCs were plated in 24-well plates at 4×10^4 cells per well in the culture medium. For contractile activity measurements, DMEM was replaced with Krebs salt solution gassed with O_2/CO_2 (95%/5%). After 5-min incubation with Krebs, cells were exposed for 2 min to 75 mM KCl in Krebs to induce contraction, followed by incubation in KCl-free Krebs. For the time-lapse study, VSMCs were kept at 37°C in an incubation chamber on a stage of an inverted microscope (TE200-S; Nikon, Florham Park, NJ). Images were captured at ×20 magnification by using a digital camera (Spot) driven by SimplePCI software package (Compix, Cranberry Township, PA). The cell length and area were determined at different time points by using Image-Pro Plus software (Media Cybernetics, Silver Spring, MD). Maximal cell shortening (contraction) was determined from 100 cells per culture from three to eight different VSMC cultures per group in triplicate. The data collector was blinded to the culture type. Cases for the study were randomly selected.

Adenoviral sh*SRF* and *MYOCD* Gene Constructs. Briefly, shuttle vectors (pENTR class vectors, Invitrogen, Carlsbad, CA) containing the U6-driven SRF RNAi cassette (27) or the indicated control, were recombined with pAd/pl-DEST (Invitrogen) by using LR clonase (Invitrogen) to create the adenoviral constructs. Large-scale adenoviral preparations were kindly provided through the University of Pittsburgh's National Heart Lung and Blood Institute-funded Vector Core Facility (Pittsburgh, PA). CMV-driven human *MYOCD* (kindly provided by Michael Parmacek, University of Pennsylvania, Philadelphia, PA) or the indicated control were similarly recombined with pAd/pl-DEST (Invitrogen) by using LR clonase (Invitrogen) to create the adenoviral construct, which was then amplified to high titer.

Gene Transfer to VSMC. For Western blot analysis of contractile proteins, 2×10^5 AD VSMCs plated in a 60-mm dish were incubated with Ad.sh*SRF* or Ad.sh*GFP* at a multiplicity of infection (moi) of 100 in DMEM/2% FBS for 2 h at room temperature with rocking. After removal of the virus, transduced AD VSMCs were cultured in DMEM for another 4 days. Age-matched control VSMCs were incubated with Ad.*MYOCD* or Ad.*GFP* at moi 100. After removal of the virus, transduced control VSMCs were cultured for 48 h. For *in vitro* contractility assay, 1×10^4 AD VSMC transduced with Ad.sh*SRF* or Ad.sh*GFP* at moi 100 or 1×10^4 control VSMCs transduced with Ad.*MYOCD* or Ad.*GFP* at moi 100 were plated in a 24-well plate, as described above.

Mouse Vascular Contractility Assay. The thoracic aorta was isolated from anesthetized (0.5 mg/kg ketamine and 5 mg/kg xylazine i.p.) 3- to 4-day-old C57BL/6J mice by using an approved institutional protocol according to National Institutes of Health guidelines. Tissue sections (3–4 mm) were placed in a 10-ml Radnoti organ bath connected to a Grass myograph (Grass-Telefactor Instruments, Warwick, RI). Tissue was bathed in Krebs buffer gassed with 95% O_2/5% CO_2 at pH 7.4, 37°C. The precontraction state of each aortic ring was determined by running a dose–response curve for phenylephrine to establish maximum contraction. For relaxation studies with acetylcholine and sodium nitroprusside, rings were precontracted with phenylephrine at 80% maximum contraction.

Transduction of Aortic Rings *ex Vivo*. Two 4-mm segments were incubated together in a 96-well plate at 37°C under 95% O_2/5% CO_2 for 2 h with viral suspension containing 2×10^8 pfu of Ad.*MYOCD* or Ad.*GFP*. GFP expression was visualized with an inverted fluorescent microscope (Nikon TE2000-S). For Western blot analysis, rings were rinsed twice with ice-cold PBS and then lysed in 25 μl of 1× SDS sample buffer. Ten microliters of lysate was run on a 6% gel for the detection of SM MHC with mouse monoclonal anti-human SM MHC (1:2,000; Upstate Biotechnology, Lake Placid, NY). β-Tubulin was used as a control for protein loading.

Transgenic Mice. We used 9-mo-old Dutch/Iowa/Swe APP (32) and 16-mo-old *APPsw*$^{+/-}$ mice (33).

***In Vivo* Transduction of Cerebral Arteries.** We modified a viral delivery technique for gene transfer to subdural arteries in rabbits by cisterna magna (49) to slow subarchnoid colony-stimulating-factor perfusion in mice for adenoviral-mediated gene transfer to subarachnoid pial neocortical arteries using an approved institutional protocol according to the National Institutes of Health guidelines. Mice were anesthetized with urethane (750 mg/kg, i.p.) and chloralose (50 mg/kg, i.p.). A small cranial window (2 × 2 mm) was made over the whisker-barrel area of the left somatosensory cortex (Brodmann's areas 1, 2, and 3). Sterilized mock colony-stimulating factor was applied to the window to avoid tissue drying. Control CBF responses to vibrissal stimulation were measured as described below. Next, a small incision was carefully made on the posterior part of the exposed dura for infusion of viral particles over the whisker-barrel area. Viral suspensions (2 μl), containing 1×10^9 pfu of Ad.*GFP* or Ad.*MYOCD* and Ad.sh*SRF* or Ad.sh*GFP* incubated in PBS and poly(L)-lysine (100 times the viral particles) to enhance transduction (49), were infused over the brain surface at 0.1 μl/min by using an infusion pump (MicroSyringe Pump, World Precision Instruments, Sarasota, FL). The window was then sealed with a glass covering slip using glue and bone wax. The mice were allowed to recover and were left for 5 days for optimum transduction (49). At the end of this period, the mice were reanesthetized, and changes in CBF due to vibrassal stimulation after gene transfer were determined as below.

CBF. We measured the CBF responses to vibrissal stimulation (7, 8) in anesthetized control, Dutch/Iowa/Swe *APP*, and *APPsw*$^{+/-}$ mice before and after transduction with control *GFP* gene or *MYOCD* or control sh*GFP* gene or sh*SRF*. CBF was determined by using laser-Doppler flowmetry (BLF 21 D; Transonic Systems, Ithaca, NY). The tip of the laser-Doppler probe was stereotaxically placed 0.5 mm above the dura of the cranial window. The right vibrissae were cut to ≈5 mm and stimulated by gentle stroking at 3–4 Hz for 1 min with a cotton-tip applicator, as described (7). The percentage increase in CBF due to vibrissal stimulation was obtained from the baseline CBF and stable maximum plateau and averaged for the three trials.

Brain Analysis After *in Vivo* Gene Transfer. Expression of GFP in the transduced brain pial arteries was confirmed by observing fluorescence on fresh-frozen brain sections (10 μm) or on isolated cerebral pial vessels by using a microscope (Nikon E600). To determine *MYOCD* mRNA, total RNA was isolated from mouse pial vessels using the RNeasy Kit (Qiagen, Valencia, CA). Conventional PCR assay was performed by using an MJ Research (Ramsey, MN) PTC-200 Peltier Thermal Cycler and Taq Polymerase (Invitrogen). Expression of SM MHC and calponin in the transduced pial vessels was determined by Western blot analysis.

Statistical Analysis. ANOVA was used to determine statistically significant differences. $P < 0.05$ was considered statistically significant.

See *SI Text* for detailed methods.

We thank Dr. Michael Parmacek for the human MYOCD expression plasmid, Ms. Margaret Parisi for preparing the illustrations, Mrs.

Xiaomei Song for assisting with immunostaining studies, and Dr. Jamila Ibrahim for performing preliminary studies on VSMC contractility. This study was supported by a Socratech L.L.C. research grant and by National Institutes of Health (NIH) grants to Socratech L.L.C. [1R43 AG024000 (to N.C.) and 1R41 AG02695001 (to J.M.M.)] and NIH Grants R37AG023084 (to B.V.Z.) and HL62572 (to J.M.M.).

1. Zlokovic BV (2005) *Trends Neurosci* 28:202–208.
2. Iadecola C (2004) *Nat Neurosci Rev* 5:347–360.
3. Greenberg SM, Gurol ME, Rosand J, Smith EE (2004) *Stroke* 35:2616–2619.
4. O'Brien JT, Erkinjuntti T, Reisberg B, Roman G, Sawada T, Pantoni L, Bowler JV, Ballard C, DeCarli C, Gorelick PB, *et al.* (2003) *Lancet Neurol* 2:89–98.
5. Casserly I, Topol E (2004) *Lancet* 353:1139–1146.
6. Redwine JM, Kosofsky B, Jacobs RE, Games D, Reilly JF, Morrison JH, Young WG, Bloom FE (2003) *Proc Natl Acad Sci USA* 100:1381–1386.
7. Iadecola C, Zhang F, Niwa K, Eckman C, Turner SK, Fischer E, Younkin S, Borchelt DR, Hsiao KK, Carlson GA (1999) *Nat Neurosci* 2:157–161.
8. Niwa K, Younkin L, Ebeling C, Turner SK, Westaway D, Younkin S, Ashe KH, Carlson GA, Iadecola C (2000) *Proc Natl Acad Sci USA* 97:9735–9740.
9. Smith CD, Andersen AH, Kryscio RJ, Schmitt FA, Kindy MS, Blonder LX, Avison MJ (1999) *Neurology* 53:1391–1396.
10. Bookheimer SY, Strojwas MH, Cohen MS, Saunders AM, Pericak-Vance MA, Mazziotta JC, Small GW (2000) *N Engl J Med* 343:450–456.
11. Ruitenberg A, den Heijer T, Bakker SL, van Swieten JC, Koudstaal PJ, Hofman A, Breteler MM (2005) *Ann Neurol* 57:789–794.
12. Mies G, Ishimaru S, Xie Y, Seo K, Hossmann KA (1991) *J Cereb Blood Flow Metab* 11:753–761.
13. Martin KC, Barad M, Kandel ER (2000) *Curr Opin Neurobiol* 10:587–592.
14. Kleim JA, Bruneau R, Calder K, Pocock D, VandenBerg PM, MacDonald E, Monfils MH, Sutherland RJ, Nader K (2003) *Neuron* 40:167–176.
15. Snowdon DA, Greiner LH, Mortimer JA, Riley KP, Greiner PA, Markesbery WR (1997) *J Am Med Assoc* 277:813–817.
16. Vermeer SE, Prins ND, den Heijer T, Hofman A, Koudstaal PJ, Breteler MM (2003) *N Engl J Med* 348:1215–1222.
17. Wang D-Z, Olson EN (2004) *Curr Opin Genet Dev* 14:558–566.
18. Miano JM (2003) *J Mol Cell Cardiol* 35:577–593.
19. Chang J, Wei L, Otani T, Youker KA, Entman ML, Schwartz RJ (2003) *Circulation* 108:407–413.
20. Kemp PR, Metcalfe JC (2000) *Biochem J* 345:445–451.
21. Belaguli NS, Zhou W, Trinh TH, Majesky MW, Schwartz RJ (1999) *Mol Cell Biol* 19:4582–4591.
22. Wang D, Chang PS, Wang Z, Sutherland L, Richardson JA, Small E, Krieg PA, Olson EN (2001) *Cell* 105:851–862.
23. Chen J, Kitchen CM, Streb JW, Miano JM (2002) *J Mol Cell Cardiol* 34:1345–1356.
24. Du KL, Ip HS, Li J, Chen M, Dandre F, Yu W, Lu MM, Owens GK, Parmacek MS (2003) *Mol Cell Biol* 23:2425–2437.
25. Yoshida T, Sinha S, Dandre F, Wamhoff BR, Hoofnagle MH, Kremer BE, Wang DZ, Olson EN, Owens GK (2003) *Circ Res* 92:856–864.
26. Wang Z, Wang D-Z, Pipes GCT, Olson EN (2003) *Proc Natl Acad Sci USA* 100:7129–7134.
27. Streb JW, Miano JM (2005) *J Biol Chem* 280:4125–4134.
28. Sun Q, Chen G, Streb JW, Long X, Yang Y, Stoeckert CJ, Jr, Miano JM (2006) *Genome Res* 16:197–207.
29. Bai N, Moien-Afshari F, Washio H, Min A, Laher I (2004) *Vasc Pharmacol* 41:97–106.
30. Li S, Wang D-Z, Richardson JA, Olson EN (2003) *Proc Natl Acad Sci USA* 100:9366–9370.
31. Miano JM, Ramanan N, Georger MA, de Mesy Bentley KL, Emerson RL, Balza RO, Jr, Xiao Q, Weiler H, Ginty DD, Misra RP (2004) *Proc Natl Acad Sci USA* 101:17132–17137.
32. Zhang X, Azhar G, Chai J, Sheridan P, Nagano K, Brown T, Yang J, Khrapko K, Borras AM, Lawitts J, *et al.* (2001) *Am J Physiol* 280:1782–1792.
33. Davis J, Xu F, Deane R, Romanov G, Previti ML, Zeigler K, Zlokovic BV, Van Nostrand WE (2004) *J Biol Chem* 279:20296–20306.
34. Holtzman DM, Fagan AM, Mackey B, Tenkova T, Sartorius L, Paul SM, Bales K, Ashe KH, Irizarry MC, Hyman BT (2000) *Ann Neurol* 47:739–747.
35. Kayed R, Head E, Thompson JL, McIntire TM, Milton SC, Cotman CW, Glabe CG (2003) *Science* 300:486–489.
36. Yoshida T, Kawai-Kowase K, Owens GK (2004) *Arterioscler Thromb Vasc Biol* 24:1596–1601.
37. Miano JM (2004) *Circ Res* 95:340–342.
38. Wu Z, Guo H, Chow N, Sallstrom J, Bell RD, Deane R, Brooks AI, Kanagala S, Rubio A, Sagare A, *et al.* (2005) *Nat Med* 11:959–965.
39. Tong L, Balazs R, Thornton PL, Cotman CW (2004) *J Neurosci* 24:6799–6809.
40. Alberti S, Krause SM, Kretz O, Philippar U, Lemberger T, Casanova E, Wiebel FF, Schwarz H, Frotscher M, Schutz G, *et al.* (2005) *Proc Natl Acad Sci USA* 102:6148–6153.
41. Etkin A, Alarcon JM, Weisberg SP, Touzani K, Huang YY, Nordheim A, Kandel ER (2006) *Neuron* 50:127–143.
42. Reynolds PR, Mucenski ML, Le Cras TD, Nichols WC, Whitsett JA (2004) *J Biol Chem* 279:37124–37132.
43. Beach TG, Wilson JR, Sue LI, Newell A, Poston M, Cisneros R, Pandya Y, Esh C, Connor DJ, Sabbagh M, Walker DG, Roher AE (2007) *Acta Neuropathol* 113:13–21.
44. Park L, Anrather J, Zhou P, Frys K, Pitstick R, Younkin S, Carlson GA, Iadecola C (2005) *J Neurosci* 25:1769–1777.
45. Braak H, Braak E (1991) *Acta Neuropathol* 82:239–259.
46. Hyman BT, Trojanowski JQ (1997) *J Neuropathol Exp Neurol* 56:1095–1097.
47. Davis J, Wagner MR, Zhang W, Xu F, Van Nostrand WE (2003) *J Biol Chem* 278:19054–19061.
48. Holland PM, Abramson RD, Watson R, Gelfand DH (1991) *Proc Natl Acad Sci USA* 88:7276–7280.
49. Toyoda K, Nakane H, Heistad DD (2001) *J Cereb Blood Flow Metab* 21:1125–1131.